

# Robno območna integralska metoda za numerično modeliranje lebdečih slojev

## Boundary Domain Integral Method for Numerical Modeling of Fluidized Beds

Matej Požarnik · Leopold Škerget

V prispevku je prikazano numerično reševanje dinamike dvo faznih dvoestavinskih tokov z robno območno integralsko metodo. Model opisa gibanja sestavin temelji na modelu dveh tekočin s hitrostno-vrtinčno formulacijo dopolnjenih Navier-Stokesovih enačb. Poseben poudarek je namenjen členu medfazne izmenjave gibalne količine. Kot testna primera sta prikazana enofazni tok v kanalu z nenasno simetrično razširivijo in dvo fazni dvoestavinski tok v navpičnem kanalu.

© 2002 Strojniški vestnik. Vse pravice pridržane.

(Ključne besede: tok dvo fazni, modeliranje numerično, metode robno-območne, metode integralske, enačbe Navier-Stokes)

The paper deals with the numerical modeling of two-phase two-component flows using the boundary domain integral method. The two-fluid model with the velocity-vorticity formulation of modified Navier-Stokes equations is adopted. Particular attention is given to the interphase momentum exchange term. As test cases a single-phase symmetric sudden expansion flow and two-phase two-component vertical channel flow are investigated.

© 2002 Journal of Mechanical Engineering. All rights reserved.

(Keywords: two phase flow, numerical modeling, boundary domain integral methods, Navier-Stokes equations)

### 0 UVOD

Lebdeči sloj sestavlja navzgor gibajoča se tekočina, ponavadi plin in na nosilno ploščo nasut sloj polnil. Kljub temu, da se trdni delci, ki hitrost plina preseže najmanjšo hitrost lebdenja, večino časa še vedno dotikajo, se mešanica plina in trdnih delcev obnaša kot tekočina. Tlak v zmesi se povečuje linearne z razdaljo pod površino, težji delci tonejo, lažji se dvigujejo, opaziti je mogoče gibanje v obliki valov. Trdne delce, ki jih imenujemo polnila, lahko stalno dodajamo ali odvzemamo. Vsa drobna polnila imajo izredno veliko specifično površino; 1 m<sup>3</sup> delcev premera 10<sup>-4</sup> m ima površino 30 000 m<sup>2</sup>. Zelo pomembno je nemirno delovanje plinskih mehurčkov, ki skrbi za popolno mešanje polnil. Posledica sta veliki toplotni in snovski prestopnosti med površino in lebdečim slojem ter med plinom in polnilu, ki povzročita, da je temperaturno in koncentracijsko polje homogeno tako v prečni kakor tudi vzdolžni smeri. Če primerjamo lebdeči sloj z nasutim slojem enakih polnil pri enaki višini sloja in hitrosti plina ugotovimo, da je tlachni padec v lebdečem sloju veliko manjši. Zaradi vsega naštetevega so lebdeči sloji oziroma dvo fazni dvoestavinski tokovi plin-trdni delci zelo privlačno procesno orodje.

### 0 INTRODUCTION

A fluidized bed is formed by passing a fluid, usually a gas, upwards through a bed of particles that are supported on a distributor. Even though above the minimum fluidization velocity the particles are touching each other most of the time the interparticle friction is so small that the fluid/solid assembly behaves like a fluid. The pressure increases linearly with the distance below the surface: denser objects sink, lighter ones float, and a wave motion is observed. Solids can be removed from or added to the bed continuously, and this provides many processing advantages. All fine powders have a very large specific surface area — 1 m<sup>3</sup> of 10<sup>-4</sup> m particles has a surface area of about 30000 m<sup>2</sup> — but in a fluidized bed the stirring action of the gas bubbles continuously moves the powder around, shearing it and exposing it to the gas. This excellent solids mixing gives the high rates of heat transfer from the surface to the bed and from the gas to particles resulting in isothermal conditions: both radially and axially. Compared with a fixed bed of the same powder operated at the same bed depth and gas velocity, the pressure drop over a fluidized bed is much smaller, and this together with most of the other characteristics make the fluidized bed an attractive choice as a chemical or physical processing tool.

Računalniška dinamika tekočin (RDT) postaja vse pomembnejše orodje za določevanje tokov v različnih vrstah industrijskih naprav. Kljub temu, da so programski paketi za modeliranje enofaznih tokov široko dosegljivi, modeliranje večfaznih sistemov še vedno pomeni veliko težavo, tako s fizikalnega kakor z numeričnega vidika. Avtorjema znani numerični algoritmi za modeliranje dvofaznih dvoestavinskih tokov brez izjeme temelijo na postopkih končnih razlik, končnih elementov oziroma kontrolnih prostornin.

V prispevku podajamo razvoj alternativne numerične sheme na podlagi robno območne integralske metode (ROIM) za reševanje splošnega primera gibanja dvofaznega dvoestavinskega sistema. Prispevek predstavlja prvi primer uporabe tako ROIM kakor tudi hitrostno-vrtinčne formulacije za modeliranje dvofaznih tokov. Kot podlago za izpeljavo dopolnjenih sistemov Navier-Stokesovih enačb smo uporabili v literaturi dobro znan model dveh tekočin (MDT). Prednost hitrostno-vrtinčne formulacije omenjenega matematičnega modela fizikalnih zakonov ohranitve mase in gibalne količine je, ob določenih dodatnih predpostavkah, numerična ločitev kinematike in kinetike toka obeh sestavin od računanja termodinamičnega tlaka in navideznega tlaka trdne snovi. Pomembna za oblikovanje hitrostnih in vrtinčnih polj sestavin je izmenjava gibalne količine med sestavinama, ki jo opišemo s koeficientom medfazne izmenjave gibalne količine.

## 1 DVOFAZNI DVOESTAVINSKI MODEL

Število delcev v lebdečem sloju realne velikosti je kljub naraščajočim računalniškim zmogljivostim preveliko, da bi z Lagrangeovo metodo modelirali gibanje vsakega delca posebej. Tak postopek omogoči študij mikroskopskih lastnosti lebdečega sloja. V prispevku prikazana shema temelji na modelu dveh tekočin, dopolnjenim s teorijo gnanega toka dvofaznih tokov. V MDT obe sestavini obravnavamo kot zvezni in medsebojno popolnoma pronicajoči. Model dveh tekočin sta prva predstavila Anderson in Jackson [1].

### 1.1 Zapis za osnovne spremenljivke

Kontinuitetno enačbo za sestavino  $p$  ( $f$  za plin in  $s$  za trdno snov) zapišemo kot:

$$\frac{\partial}{\partial t} (\varepsilon_p \rho_p) + \frac{\partial}{\partial x_j} (\varepsilon_p \rho_p v_{pj}) = 0 \quad \text{in/and} \quad \sum_{p=f,s} \varepsilon_p = 1 \quad (1).$$

Izmenjava snovi med sestavinama, npr. zaradi kemijske reakcije ali zgorevanja, ni zajeta.

Gibalna enačba plinaste sestavine je podana kot dopolnjena Navier-Stokesova enačba, ki vsebuje člen medfazne izmenjave gibalne količine:

$$\frac{Dv_{fi}}{Dt} = \frac{1}{\rho_f \varepsilon_f} \frac{\partial S_{fij}}{\partial x_j} + g_i - \frac{1}{\rho_f} \frac{\partial p}{\partial x_i} - \frac{\beta}{\rho_f \varepsilon_f} (v_{fi} - v_{si}) \quad (2).$$

Computational fluid dynamics (CFD) is becoming an increasingly common engineering tool to predict flows in various types of apparatus on an industrial scale. Although the tools for applying single-phase CFD are widely available, the application of multiphase CFD is still complicated from both the physical and the numerical points of view. All the numerical algorithms known to the authors that were developed so far to simulate two-phase two-component flows are strictly based on the finite-difference method, the finite-element method or the control-volume method.

In this paper an alternative numerical scheme based on the boundary domain integral method (BDIM) is presented for the solution of a general two-phase two-component flow motion problem. This is definitely the first attempt to implement the BDIM and velocity-vorticity formulation for modeling two-phase flows. The two-fluid model (TFM) is used to derive two sets of modified Navier-Stokes equations. The velocity-vorticity formulation of the physical conservation laws of mass and momentum then follows. The advantages of this approach lie with the numerical separation of kinematic and kinetic aspects of both phases motion from the thermodynamic pressure and the solid's pressure computation. Particular attention is given to the drag between the phases, which is described by the interphase momentum exchange coefficient.

## 1 TWO-PHASE TWO-COMPONENT MODEL

In spite of increasing computational power the number of particles in a gas-solid flow in large scale equipment is still much too large to handle each particle separately. Simulating each particle separately is called a Lagrangian method, which can be used to study the microscopic properties of fluidized beds. The CFD model used in this work is based on a TFM that is extended with the drift-flux theory of a two-phase flow. In a TFM both phases are considered to be continuous and fully interpenetrating. The TFM was first proposed by Anderson and Jackson [1].

### 1.1 Primitive variables formulation

The continuity equation or mass balance for phase  $p$  ( $f$  for gas and  $s$  for solid) reads:

Mass exchange between the phases, e.g. due to reaction or combustion, is not considered.

The momentum balance for the gas phase is given by the Navier-Stokes equation, which is modified to include an interphase momentum transfer term:

Gibalna enačba trdne snovi je podana z:

$$\frac{Dv_{si}}{Dt} = \frac{1}{\varrho_s \varepsilon_s} \frac{\partial S_{sij}}{\partial x_j} + g_i - \frac{1}{\varrho_s \varepsilon_s} \frac{\partial p_s^*}{\partial x_i} - \frac{1}{\varrho_s} \frac{\partial p}{\partial x_i} + \frac{\beta}{\varrho_s \varepsilon_s} (v_{fi} - v_{si}) \quad (3),$$

kjer je  $p_s^*$  navidezni tlak trdne snovi, ki je določen z uporabo kinetične teorije zrnatega toka. V tenzorju strižnih napetosti moramo v splošnem upoštevati tako strižno kakor tudi normalno viskoznost [2].

Z  $\varepsilon_f = 1$  in  $\beta = 0$  postane enačba (2) običajna Navier–Stokesova enačba. Kontinuitetni in gibalni enačbi sta podrobno predstavljeni v [3].

## 1.2 Hitrostno-vrtinčna formulacija

Za uporabo v predlagani shemi na podlagi ROIM originalna sistema dopolnjenih Navier–Stokesovih enačb nadalje preoblikujemo z uporabo hitrostno-vrtinčne formulacije. Na tak način računsko shemo gibanja plina in trdne snovi razdelimo na kinematični in kinetični vidik. V primeru uporabe hitrostno-vrtinčne formulacije za modeliranje enofaznih tokov iz numerične sheme izločimo računanje tlaka. Postopek vodi v primerjavi z običajnim k preprostejšemu predpisovanju robnih pogojev predvsem na tistih robovih območja, kjer tlak ni znan. Izpeljani algoritem na podlagi hitrostno-vrtinčne formulacije je kljub vsemu še vedno mogoče zapisati popolnoma splošno za modeliranje dvo-in tridimenzionalnih tokov.

Računsko shemo gibanja obeh sestavin razdelimo na kinematični in kinetični vidik z vpeljavo vektorjev vrtinčnosti  $\omega_{pi}$ , ki predstavljata rotorja hitrostnih polj. Z uporabo operatorja rotor neposredno na definiciji vrtinčnosti in upoštevanjem preoblikovane kontinuitetne enačbe (1) z  $\varepsilon_p = \text{konst.}$ :

$$\frac{\partial v_{pj}}{\partial x_j} = -\frac{1}{\varepsilon_p} \left( \frac{\partial \varepsilon_p}{\partial \tau} + v_{pj} \frac{\partial \varepsilon_p}{\partial x_j} \right) \quad (4)$$

izpeljemo kinematiko gibanja plinaste in trdne snovi:

$$\frac{\partial v_{pi}}{\partial x_j} + e_{ijk} \frac{\partial \omega_{pk}}{\partial x_j} = \frac{\partial}{\partial x_i} \left[ -\frac{1}{\varepsilon_p} \left( \frac{\partial \varepsilon_p}{\partial \tau} + v_{pj} \frac{\partial \varepsilon_p}{\partial x_j} \right) \right] \quad (5).$$

Enačba (5) podaja kinematiko gibanja nestisljive tekočine in trdnih delcev oziroma združljivost hitrostnih in vrtinčnih polj v dani točki prostora in časa.

Kinetiko podamo s prenosnima enačbama vrtinčnosti, ki pomenita rotor gibalnih enačb (2) in (3). V primeru majhnih prostorninskih deležev trdnih delcev v toku lebdečega sloja uporabimo postopek Chapman in Cowlinga [4] z nespremenljivima strižno in normalno viskoznostjo. Prenosni enačbi vrtinčnosti zapišemo kot:

$$\begin{aligned} \frac{D\omega_{fi}}{Dt} &= \nu_f \frac{\partial \omega_{fi}}{\partial x_j} - \omega_{fi} \frac{\partial v_{fj}}{\partial x_j} + \omega_{fj} \frac{\partial v_{fi}}{\partial x_j} - \frac{\beta}{\varrho_f \varepsilon_f} (\omega_{fi} - \omega_{si}) - \frac{\nu_f}{\varepsilon_f} \frac{\partial \varepsilon_f}{\partial x_j} \left( e_{ijk} e_{klm} \frac{\partial \omega_{fl}}{\partial x_m} \right) + \\ &+ \frac{4}{3} \frac{1}{\varepsilon_f} \nu_f e_{ijk} \frac{\partial v_{fl}}{\partial x_j} \frac{\partial \varepsilon_f}{\partial x_k} - \frac{\beta}{\varrho_f \varepsilon_f} e_{ijk} (v_{fj} - v_{sj}) \frac{\partial \varepsilon_f}{\partial x_k} \end{aligned} \quad (6),$$

The solid-phase momentum balance is given by:

where  $p_s^*$  is the solids pressure, originally obtained from the kinetic theory of the granular flow. Both the shear and bulk viscosities should be used in a viscous strain-rate tensor, in general [2].

With  $\varepsilon_f = 1$  and  $\beta = 0$  Eqn. (2) becomes the classical Navier–Stokes equation. The mass and momentum balances are discussed in detail in [3].

## 1.2 Velocity-vorticity variables formulation

In BDIM the original sets of Navier–Stokes equations for the gas phase and the solid particles are further transformed with the use of the velocity-vorticity variables formulation. Within this approach the flow field computation is decoupled into flow kinematics and flow kinetics. The main advantages of this scheme in the case of single-phase flow lie with the numerical separation of the kinematic and kinetic aspects of the flow from the pressure computation. This leads to a simpler way of enforcing the proper boundary conditions than the primitive variables approach whenever the pressure is not specified on the boundary as a known quantity. The developed algorithm can still be written in a general form for both two and three dimensions.

With the vorticity vector  $\omega_{pi}$ , representing the curl of the velocity field, the two phases motion computation scheme is partitioned into its kinematic and kinetic aspects. By taking the curl operator directly to the vorticity vector definition, and applying the reformed continuity Eqn. (1) with  $\varepsilon_p = \text{const.}$ :

$$\text{the kinematics of both phases motion is carried out:}$$

Eqn. (5) represents the kinematics of an incompressible fluid and solid-phase motion or the compatibility of the velocity and vorticity fields at a given point in space and time.

The kinetics are governed by the vorticity transport equations obtained as a curl of the momentum balances, Eqns. (2) and (3). In the case of low solid concentrations the approach of Chapman and Cowling [4] with constant viscosities is applied. The vorticity transport equations can be written in the following form:

$$\frac{D\omega_{si}}{Dt} = \nu_s \frac{\partial \omega_{si}}{\partial x_j} - \omega_{si} \frac{\partial v_{sj}}{\partial x_j} + \omega_{sj} \frac{\partial v_{si}}{\partial x_j} + \frac{\beta}{\varrho_s \varepsilon_s} (\omega_{fi} - \omega_{si}) - \frac{\nu_s}{\varepsilon_s} \frac{\partial \varepsilon_s}{\partial x_j} \left( e_{ijk} e_{klm} \frac{\partial \omega_{sl}}{\partial x_m} \right) + \\ + \frac{1}{\varepsilon_s} \left( \frac{4}{3} \nu_s + \kappa_s \right) e_{ijk} \frac{\partial v_{sl}}{\partial x_j} \frac{\partial \varepsilon_s}{\partial x_k} - \frac{1}{\varrho_s \varepsilon_s} e_{ijk} \frac{\partial p_s^*}{\partial x_j} \frac{\partial \varepsilon_s}{\partial x_k} + \frac{\beta}{\varrho_s \varepsilon_s} e_{ijk} (v_{fj} - v_{sj}) \frac{\partial \varepsilon_s}{\partial x_k} \quad (7),$$

ki podajata porazdelitev vektorjev vrtinčnosti plinaste sestavine in trdne snovi. Z opisanim postopkom iz izračuna izločimo termodinamični tlak  $p$ , vendar enačba (7) še vedno vsebuje gradient navideznega tlaka trdne snovi  $p_s^*$ . Zaradi tega predlagana shema temelji na tehniki podobmočij v njeni skrajni izvedenki, kar pomeni, da je vsaka celica podobmočje, imenovano makroelement, ki je omejeno s štirimi robnimi elementi. S predpostavljenim nespremenljivim prostorninskim deležem sestavine  $\varepsilon_p$  znotraj posamezne iteracije po vsakem izmed makroelementov zagotovimo, da gradient prostorninskega deleža po območju ne obstaja ( $\partial \varepsilon_p / \partial x_j = 0$ ). Z upoštevanjem primernih vmesnih pogojev na mejah med makroelementi, ki so podrobnejše predstavljeni v poglavju 1.4, enačbe (5), (6) in (7) zapišemo v poenostavljeni obliki.

Po predpostavki glede prostorninskega deleža  $\varepsilon_p$  kinematiko gibanja obeh sestavin zapišemo v obliki parabolične enačbe z uporabljenim nepravim neustaljenim načinom:

$$\frac{\partial v_{pi}}{\partial x_j} - \frac{1}{\alpha_p} \frac{\partial v_{pi}}{\partial \tau} + e_{ijk} \frac{\partial \omega_{pk}}{\partial x_j} = 0. \quad (8).$$

Transportni enačbi vrtinčnosti, enačbi (6) in (7), prepišemo v naslednjo obliko:

$$\frac{D\omega_{fi}}{Dt} = \nu_f \frac{\partial \omega_{fi}}{\partial x_j} + \frac{\omega_{fi}}{\varepsilon_f} \frac{\partial \varepsilon_f}{\partial \tau} + \omega_{ff} \frac{\partial v_{fi}}{\partial x_j} - \frac{\beta}{\varrho_f \varepsilon_f} (\omega_{fi} - \omega_{si}) \quad (9),$$

$$\frac{D\omega_{si}}{Dt} = \nu_s \frac{\partial \omega_{si}}{\partial x_j} + \frac{\omega_{si}}{\varepsilon_s} \frac{\partial \varepsilon_s}{\partial \tau} + \omega_{sj} \frac{\partial v_{si}}{\partial x_j} + \frac{\beta}{\varrho_s \varepsilon_s} (\omega_{fi} - \omega_{si}) \quad (10).$$

Enačbi (9) in (10) podajata v primeru tridimenzionalnih tokov časovno spremembo vrtinčnosti delca plina oziroma trdne snovi, podano s Stokesovim odvodom na levi strani enačb, zaradi učinkov viskozne difuzije, nastajanja mehurjev, učinkov deformacije in medfazne izmenjave gibalne količine, podane s členi na desni strani enačb.

### 1.3 Prostorninski delež

Za sklenitev sistema kinematičnih in kinetičnih enačb gibanja sestavin dvofaznega dvoestavinskega toka potrebujemo dodatno enačbo za izračun prostorninskega deleža plinaste sestavine. Izpeljemo jo iz teorije gnanega toka dvofaznih tokov [9]. Teorija je izpeljana splošno in obsega različnost fizikalnih lastnosti in tokovnih polj dvofaznega toka. Omogoča zapis ločenih kontinuitetnih in gibalnih enačb za vsako sestavino posebej. Uporabna je za modeliranje različnih režimov dvofaznih tokov plin - kapljevina kakor tudi za modeliranje dvofaznih dvoestavinskih sistemov tekočina - trdni delci, npr.

describing the redistribution of the vorticity vector in the fluid and solid particles' flow field. While the thermodynamic pressure  $p$  is not part of the computation, Eqn. (7) is still dealing with the solids pressure  $p_s^*$  gradient. Therefore, the proposed numerical scheme is based on the subdomain technique in its limit version. Each internal cell represents one subdomain called a macroelement, which is bounded by four boundary elements. The macroelement volume fraction of a phase  $\varepsilon_p$  is assumed to be constant within a particular iteration of the numerical algorithm, therefore, in that moment the gradient  $\partial \varepsilon_p / \partial x_j = 0$  does not exist all over the macroelement. Then the Eqns. (5), (6), and (7) can be rewritten in a simple manner, but a lot of the physics is moved to the macroelement interface boundary conditions explained in detail in section 1.4.

After the assumption regarding the volume fraction  $\varepsilon_p$  the kinematics of both phases motion is written in the sense of the parabolic equation where the false transient approach is implemented afterwards:

Using the same principle the kinetics given by Eqns. (6) and (7) is rewritten as:

Eqns. (9) and (10) show that the rate of change of the vorticity in the case of 3D flow as one follows a fluid or solid particle, given by the Stokes derivation on the left-hand side of the equations, is due to the viscous diffusion, bubble formation, vortex twisting and stretching, and interphase-momentum transfer, represented by the terms on the right-hand side.

### 1.3 Volume fraction

To close the system of kinematics and kinetics equations an additional equation to compute the volume fraction of the fluid phase is derived from the drift flux theory of the two-phase flow [9]. This model treats the general case of modelling each phase or component as a separate fluid with its own set of governing balance equations. In general, each phase has its own velocity, vorticity, and temperature. Drift-flux theory has widespread application in the bubbly, slug, and drop regimes of gas-liquid flow as well as to fluid-particle systems such as fluidized beds. It provides a starting point for the extension of the

lebdeči sloji. Namenjena je tudi kot izhodišče za preučevanje tokov s prevladajočimi 2D in 3D vplivi. Prostorninski delež sestavine določimo z enačbo:

$$\varepsilon_f = \sqrt[n-1]{\frac{|v_{fi} - v_{si}|}{|v_{\infty}|}}, \quad (11),$$

kjer je  $v_{\infty}$  Stokesova hitrost posameznega trdnega delca v mirujoči tekočini. Določitev vrednosti koeficiente  $n$  podajata Richardson in Zaki [7]. Celotna korelacija Richardsona in Zakiha za vse vrednosti Reynoldsovega števila podaja vrednosti  $n$  med 4,65 in 2,39, upoštevajoč, da so trdni delci toge kroglice majhnega premera v primerjavi z izmerami kanala. Vrednost koeficiente  $n$  lahko še povečamo, če prihaja do združevanja delcev. V predstavljeni raziskavi uporabljamo srednjo vrednost koeficiente  $n$  za sisteme plin - trdni delci ( $n=3$ ). Vpeljati je mogoče tudi korekcijski faktor v odvisnosti od razmerja med premerom delcev in izmerami kanala.

#### 1.4 Pogoji vmesnega roba

Kadar zapišemo dopolnjen sistem Navier-Stokesovih enačb gibanja dvofaznega dvoestavinskega sistema za nespremenljiv prostorninski delež sestavine v podobmočju v iteraciji numeričnega algoritma, so najbolj kritičen del izračuna pogoji vmesnega roba na mejah med makroelementi. Zaradi tega smo posebno pozornost namenili analizi nezveznosti. Vektorje hitrosti razdelimo na normalno in obodno komponento glede na rob podobmočja. Zaradi predpisanega nespremenljivega prostorninskega deleža znotraj posamezne iteracije je glavna značilnost vmesnega roba  $\Gamma_l$  med podobmočjema  $\Omega_l$  in  $\Omega_2$  skok prostorninskega deleža sestavine in posledično tudi skok normalne komponente hitrosti. Obodne komponente vektorjev hitrosti se spreminjajo zvezno. Za gibanje v ravnini  $x$ - $y$  velja naslednja povezava med normalnimi in tangentnimi odvodi normalne in obodne komponente vektorja hitrosti:

$$\omega_p = \frac{\partial v_{pt}}{\partial n} - \frac{\partial v_{pn}}{\partial t} \quad (12).$$

Iz ohranitvenih zakonov izpeljemo ustrezne pogoje vmesnega roba kinematike:

$$v_{pt}|_{\bar{\Gamma}} = -v_{pt}|_{\bar{\Gamma}} \quad (13),$$

$$v_{pn}\varepsilon_p|_{\bar{\Gamma}} = -v_{pn}\varepsilon_p|_{\bar{\Gamma}} \quad (14),$$

$$\frac{\partial v_{pt}}{\partial n}|_{\bar{\Gamma}} = \frac{\partial v_{pt}}{\partial n}|_{\bar{\Gamma}} \quad (15),$$

$$\varepsilon_p \frac{\partial v_{pn}}{\partial n}|_{\bar{\Gamma}} = \varepsilon_p \frac{\partial v_{pn}}{\partial n}|_{\bar{\Gamma}} \quad (16)$$

in kinetike

and for the kinetics are:

$$\omega_p|_{\bar{\Gamma}} = \omega_p|_{\bar{\Gamma}} + \left(1 - \frac{\varepsilon_p^-}{\varepsilon_p^+}\right) \frac{\partial v_{pn}}{\partial t}|_{\bar{\Gamma}} \quad (17),$$

theory to flows in which two- and three-dimensional effects are significant. The volume fraction of the component is determined by following equation:

where  $v_{\infty}$  is the terminal speed of a single solid particle in an infinite stationary liquid. The evaluation of index  $n$  was shown by Richardson and Zaki [7]. The complete correlation of Richardson and Zaki over the whole range of Reynolds numbers gives a value for the index  $n$  between 4,65 and 2,39, assuming that the particles are rigid spheres and small compared to the diameter of the channel. The value of  $n$  can also be enlarged when the particles flocculate. In our study only small Reynolds number flow is encountered, therefore, an intermediate value of the index  $n$  for fluid-particle systems is taken into account ( $n=3$ ). A correction factor can also be introduced in terms of the ratio of the particle diameter to the tube diameter.

#### 1.4 Macroelement interface boundary conditions

When dealing with the modified Navier-Stokes system of equations written for the constant volume fraction of the component over each macroelement within a particular iteration the most critical parts of the numerical scheme are the macroelement interface boundary conditions. Therefore, particular attention has been given to the analysis of a jump discontinuity in the flow properties. Velocity vectors at the macroelement interface boundaries are split into normal and tangential components. The major interface characteristics are a jump in the volume fraction and the continuity of the tangential velocity (no-slip). Due to the volume fraction jump the jump in normal velocity is also necessary. For the macroelement interface the relation relating the vorticity values with the normal and tangential velocity component fluxes is derived. For two-dimensional motion in the  $x$ - $y$  plane it reads:

Appropriate macroelement interface boundary conditions derived from the conservation laws for the kinematics are:

$$\frac{\partial \omega_p}{\partial n}|_{\bar{I}} = -\frac{\partial \omega_p}{\partial n}|_{\bar{I}} - \left(1 - \frac{\varepsilon_p}{\varepsilon_p}\right) \frac{\partial v_{pn}}{\partial n \partial t}|_{\bar{I}} \quad (18).$$

S predpisanim  $\varepsilon_p = 1$  na obeh straneh vmesnega roba  $\Gamma_I$  med podobmočjema  $\Omega_1$  in  $\Omega_2$  enačbe od (13) do (18) privzamejo običajno obliko pogojev vmesnega roba za enofazno gibanje viskozne nestisljive tekočine.

### 1.5 Robni pogoji

Za numerično rešitev sistema enačb gibanja dvofaznega dvoestavinskega toka plin - trdna snov je treba predpisati primerne robne pogoje za obe sestavini. Običajni robni pogoji v primeru zapisa za osnovne spremenljivke so znane vrednosti robnih hitrosti obeh sestavin, termodinamični tlak plinaste sestavine in navidezna temperatura trdne snovi, ki je izpeljana iz kinetične teorije zrnatega toka in je namenjena za določitev navideznega tlaka trdne snovi. Pri zapisu za hitrostno-vrtinčno formulacijo potrebujemo za obe sestavini le znane vrednosti robnih hitrosti oziroma vrednosti njihovih odvodov. Robni pogoji običajne ROIM so podrobno predstavljeni v [8].

Na neporozni trdni steni kanala pri toku plina in trdnih delcev predpišemo po navadi brezzdrsne robne pogoje plinaste sestavine. Tega ne moremo vedno storiti tudi za trdne delce, saj pri toku delcev večjega premera v primerjavi s hrapavostjo sten prihaja do zdrsa pri trku ob steno. Mnogokrat kljub temu predpostavimo, da so delci izjemno majhni, kar omogoči predpisovanje brezzdrsnih robnih pogojev tudi za trdno snov. Začetni pogoji prostorninskega deleža sestavin lahko zavzamejo katerokoli fizikalno sprejemljivo vrednost.

## 2 INTEGRALSKA PREDSTAVITEV HITROSTNO-VRTINČNE FORMULACIJE DVOFAZNEGA DVOESTAVINSKEGA TOKA

### 2.1 Kinematika gibanja plina in trdne snovi

Pri obravnavi kinematike obeh sestavin v robno-območni integralski predstavitev upoštevamo, da vsaka komponenta vektorjev hitrosti v enačbi (8) zadošča nehomogeni parabolični enačbi:

$$\alpha_p \frac{\partial v_{pi}}{\partial x_j \partial x_j} - \frac{\partial v_{pi}}{\partial \tau} + b_{pi} = 0 \quad (19).$$

Z enačenjem vektorja navidezne telesne sile  $b_{pi}$  z vrtinčnim delom toka obeh sestavin:

$$b_{pi} = \alpha_p \epsilon_{ijk} \frac{\partial \omega_{pk}}{\partial x_j} \quad (20)$$

zapišemo pripadajoč integralski izraz:

where subscript  $I$  denotes the interface boundary  $\Gamma_I$  between the macroelements  $\Omega_1$  and  $\Omega_2$ . With  $\varepsilon_p = 1$  at both sides of the boundary  $\Gamma_I$  the Eqns. from (13) to (18) take on the classical form for single-phase fluid motion.

### 1.5 Boundary conditions

To solve the equations for gas-solid particles flow we need appropriate boundary conditions, not only for the fluid phase but also for the solid particles. Classical boundary conditions in the case of primitive variables formulation are the velocities of the gas phase and the solid particles, the boundary condition for gas-phase pressure and the boundary granular temperature derived from the kinetic theory of granular flow to compute the solids pressure. In the velocity-vorticity variables approach we need only the appropriate boundary conditions for the velocities or velocity fluxes of the gas and the solids. The boundary conditions for the classical BDIM approach are discussed in detail in [8].

For the gas-solid particle flow motion the gas-phase velocities are generally set to zero at an impenetrable rigid wall. This no-slip condition cannot always be applied to solid motion. Since the particle diameter is usually larger than the length scale of the surface roughness of the rigid wall, the particles may partially slip the wall. But it is also important to note that for small particle diameters the boundary condition is close to the no-slip condition. Initially, in a mixture of gas phase and solid particles the volume fraction of the two phases can be set to any physically acceptable value.

## 2 INTEGRAL REPRESENTATION OF THE VELOCITY-VORTICITY FORMULATION FOR TWO-PHASE TWO-COMPONENT FLOW

### 2.1 Gas and solid phase kinematics

Considering first the kinematics of both phases motion in the boundary domain integral representation one has to take into account that each component of the velocity vector in Eqn. (8) obeys the nonhomogeneous parabolic equation:

Equating the body force term  $b_{pi}$  to the vortical fluid or solid particles flow term:

renders an integral statement :

$$\begin{aligned} c(\xi) v_{pi}(\xi, \tau_F) + \alpha_p \int_{\tau_{F-1}}^{\tau_F} \int v_{pi} \frac{\partial u_p^*}{\partial n} d\tau d\Gamma &= \alpha_p \int_{\tau_{F-1}}^{\tau_F} \left( \frac{\partial v_{pi}}{\partial n} - e_{ijk} \omega_{pj} n_k \right) u_p^* d\tau d\Gamma \\ &+ \alpha_p \int_{\tau_{F-1}}^{\tau_F} \int e_{ijk} \omega_{pj} \frac{\partial u_p^*}{\partial x_k} d\tau d\Omega + \int v_{pi,F} u_{p,F}^* d\Omega \end{aligned} \quad (21),$$

kjer je  $u_p^*$  parabolična difuzijska osnovna rešitev. Če predpostavimo nespremenljiv potek vseh funkcij polja po posamičnem časovnem koraku, lahko časovne integrale v enačbi (21) rešimo analitično [8], tako da integralski stavek podamo v obliki:

$$\begin{aligned} c(\xi) v_{pi}(\xi, \tau_F) + \int v_{pi} \frac{\partial U_p^*}{\partial n} d\Gamma &= \int \left( \frac{\partial v_{pi}}{\partial n} - e_{ijk} \omega_{pj} n_k \right) U_p^* d\Gamma \\ &+ \int e_{ijk} \omega_{pj} \frac{\partial U_p^*}{\partial x_k} d\Omega + \int v_{pi,F} u_{p,F}^* d\Omega \end{aligned} \quad (22),$$

kjer je  $U_p^* = \alpha_p u_p^*$ .

## 2.2 Kinetika gibanja plina in trdne snovi

Integralsko predstavitev kinetike gibanja plina in trdne snovi zapišemo z uporabo difuzivno-konvektivne osnovne rešitve. Časovne odvode vrtinčnosti in prostorninskih deležev aproksimiramo z nesimetričnimi končnimi razlikami. Tak način omogoči zapis enačb (9) in (10) v obliki nehomogene difuzivno-konvektivne parcialne diferencialne enačbe:

$$\nu_{p-} \frac{\partial \omega_{pi}}{\partial x_j} - \frac{\partial \bar{v}_{pj} \omega_{pi}}{\partial x_j} - \frac{1}{\Delta \tau} \omega_{pi} + b_{pi} = 0. \quad (23).$$

Diferencialni zapis preoblikujemo v ustrezen integralski stavek:

$$c(\xi) \omega_{pi}(\xi) + \int \omega_{pi} \frac{\partial U_p^*}{\partial n} d\Gamma = \frac{1}{\nu_{p-}} \int \left( \nu_{p-} \frac{\partial \omega_{pi}}{\partial n} - \omega_{pi} \bar{v}_{pn} \right) U_p^* d\Gamma + \frac{1}{\nu_{p-}} \int b_{pi} U_p^* d\Omega \quad (24)$$

z  $U_p^* = \nu_{p0} \cdot u_p^*$  in  $\bar{v}_{pn} = \bar{v}_{pj} \cdot n_j$ .  $u_p^*$  je difuzivno-konvektivna osnovna rešitev. Izraz navideznih telesnih sil  $b_{pi}$  vsebuje konvekcijo zaradi spreminjačega se dela vektorja hitrosti  $\tilde{v}_{pj}$ , deformacijo, začetne pogoje, spremembo vrtinčnosti zaradi oblikovanja mehurjev in medfazne izmenjave gibalne količine:

$$b_{pi} = - \frac{\partial \bar{v}_{pj} \omega_{pi}}{\partial x_j} + \frac{\partial \omega_{pj} v_{pi}}{\partial x_j} + \frac{\omega_{pi,F}}{\Delta \tau} + \frac{\omega_{pi}}{\varepsilon_p \Delta \tau} (\varepsilon_{p,F} - \varepsilon_{p,F}) \mp \beta (\omega_{fi} - \omega_{si}) \quad (25).$$

Končni integralski stavek se glasi:

where  $u_p^*$  is the parabolic diffusion fundamental solution. Assuming a constant variation of all field variables within the individual time increment, the time integrals in Eqn. (21) may be evaluated analytically [8]. An integral statement can be finally written in the following form:

being  $U_p^* = \alpha_p u_p^*$ .

## 2.2 Gas and solid phase kinetics

An integral representation describing the kinetics of both components motion is formulated by using the fundamental solution of a steady diffusion-convective partial differential equation with a reaction term. In the case of kinetics the volume fraction and the vorticity time derivatives are approximated by using a non-symmetric finite-difference approximation. Therefore, Eqns. (9) and (10) can be rewritten as a non-homogeneous diffusion-convective partial differential equation:

The above differential formulation can be transformed into an equivalent integral statement:

with  $U_p^* = \nu_{p0} \cdot u_p^*$  and  $\bar{v}_{pn} = \bar{v}_{pj} \cdot n_j$ .  $u_p^*$  is the fundamental solution of the diffusion-convective equation. The pseudo-body term  $b_{pi}$  includes the convective flux for the perturbated velocity field  $\tilde{v}_{pj}$ , deformation, initial conditions, vorticity change on account of the bubble formation and interphase momentum exchange term, for example:

The final integral representation is as follows:

$$\begin{aligned} c(\xi) \omega_{pi}(\xi) + \int \omega_{pi} \frac{\partial U_p^*}{\partial n} d\Gamma &= \frac{1}{\nu_{p-}} \int \left( \nu_{p-} \frac{\partial \omega_{pi}}{\partial n} - \omega_{pi} \bar{v}_{pn} + \omega_{pn} v_{pi} \right) U_p^* d\Gamma \\ &+ \frac{1}{\nu_{p-}} \int (\omega_{pi} \bar{v}_{pj} - v_{pi} \omega_{pj}) \frac{\partial U_p^*}{\partial x_j} d\Omega \mp \frac{\beta}{\varrho_p \varepsilon_p} \int (\omega_{fi} - \omega_{si}) U_p^* d\Omega \\ &+ \frac{1}{\nu_p \Delta \tau} \int \omega_{pi,F} U_p^* d\Omega + \frac{1}{\varepsilon_p \nu_p \Delta \tau} \int \omega_{pi} (\varepsilon_{p,F} - \varepsilon_{p,F}) U_p^* d\Omega. \end{aligned} \quad (26).$$

### 3 NUMERIČNA REŠITEV

#### 3.1 Diskretizirane enačbe

Za numerično približno rešitev obravnavanih funkcij polja, npr. hitrosti in vrtinčnosti obeh sestavin, moramo pripadajoče robno-območne integralske predstavitev zapisati v diskretni obliki. Diskretizacijo integralskih predstavitev hitrosti in vrtinčnosti obeh sestavin izpeljemo iz pripadajočih integralskih enačb (22) in (26), za kinematiko:

$$\begin{aligned} c(\xi) v_{pi}(\xi, \tau_F) + \sum_{e=1}^E \{h_{pe}\}^T \{v_{pi}\}^n &= \sum_{e=1}^E \{g_{pe}\}^T \left\{ \frac{\partial v_{pi}}{\partial n} + e_{ijk} \omega_{pk} n_j \right\}^n - \\ &- e_{ijk} \sum_{e=1}^C \{d_{pej}\}^T \{\omega_{pk}\}^n + \\ &+ \sum_{e=1}^C \{b_{pe}\}^T \{v_{pi,F}\}^n \end{aligned} \quad (27)$$

in kinetiko

$$\begin{aligned} c(\xi) \omega_{pi}(\xi) + \sum_{e=1}^E \{H_{pe}\}^T \{\omega_{pi}\}^n &= \frac{1}{\nu_{p_e}} \sum_{e=1}^E \{G_{pe}\}^T \left\{ \nu_{p_e} \frac{\partial \omega_{pi}}{\partial n} - \omega_{pi} v_{pn} + \omega_{pn} v_{pi} \right\}^n + \\ &+ \frac{1}{\nu_{p_e}} \sum_{e=1}^C \{D_{pej}\}^T \{\omega_{pi}\}_{pj}^n + \\ &+ \frac{1}{\nu_{p_e} \Delta \tau} \sum_{e=1}^C \{B_{pe}\}^T \{\omega_{pi,F}\}^n + \\ &+ \frac{1}{\nu_{p_e} \Delta \tau} \sum_{e=1}^C \{B_{pe}\}^T \{\omega_{pi}\}^n - \\ &- \frac{1}{\nu_{p_e} \varepsilon_s \Delta \tau} \sum_{e=1}^C \{B_{pe}\}^T \{\omega_{pi} \varepsilon_{p,F}\}^n \mp \\ &\mp \frac{\beta}{\rho_p \varepsilon_p} \sum_{e=1}^C \{B_{pe}\}^T \{\omega_{fi} - \omega_{si}\}^n \end{aligned} \quad (28)$$

kjer nadpis  $T$  označuje transpozicijo.

Kinematiko ravninskega toka ( $i,j=1,2$ ) podamo z naslednjim stavkom po enačbi (27):

$$\begin{aligned} c(\xi) v_{pi}(\xi, \tau_F) + \sum_{e=1}^E \{h_{pe}\}^T \{v_{pi}\}^n &= \sum_{e=1}^E \{g_{pe}\}^T \left\{ \frac{\partial v_{pi}}{\partial n} + e_{ij} \omega_{pj} n_j \right\}^n - \\ &- e_{ij} \sum_{e=1}^C \{d_{pej}\}^T \{\omega_{pj}\}^n + \\ &+ \sum_{e=1}^C \{b_{pe}\}^T \{v_{pi,F}\}^n \end{aligned} \quad (29)$$

Diskretizirane transportne enačbe vrtinčnosti obeh sestavin ravninskega toka so:

$$\begin{aligned} c(\xi) \omega_p(\xi) + \sum_{e=1}^E \{H_{pe}\}^T \{\omega_p\}^n &= \frac{1}{\nu_{p_e}} \sum_{e=1}^E \{G_{pe}\}^T \left\{ \nu_{p_e} \frac{\partial \omega_p}{\partial n} - \omega_p v_{pn} \right\}^n + \\ &+ \frac{1}{\nu_{p_e}} \sum_{e=1}^C \{D_{pej}\}^T \{\omega_p\}_{pj}^n + \\ &+ \frac{1}{\nu_{p_e} \Delta \tau} \sum_{e=1}^C \{B_{pe}\}^T \{\omega_{p,F}\}^n + \\ &+ \frac{1}{\nu_{p_e} \Delta \tau} \sum_{e=1}^C \{B_{pe}\}^T \{\omega_p\}^n - \\ &- \frac{1}{\nu_{p_e} \varepsilon_s \Delta \tau} \sum_{e=1}^C \{B_{pe}\}^T \{\omega_p \varepsilon_{p,F}\}^n \mp \\ &\mp \frac{\beta}{\rho_p \varepsilon_p} \sum_{e=1}^C \{B_{pe}\}^T \{\omega_f - \omega_s\}^n \end{aligned} \quad (30)$$

### 3 NUMERICAL SOLUTION

#### 3.1 Discretized equations

Consider a discretized equation set for the case of both fluid and solid particles motion. The discretization of the integral representations for velocities and vorticities can be readily obtained from the corresponding integral Eqns. (22) and (26) as follows, for the kinematics:

$$\begin{aligned} c(\xi) v_{pi}(\xi, \tau_F) + \sum_{e=1}^E \{h_{pe}\}^T \{v_{pi}\}^n &= \sum_{e=1}^E \{g_{pe}\}^T \left\{ \frac{\partial v_{pi}}{\partial n} + e_{ijk} \omega_{pk} n_j \right\}^n - \\ &- e_{ijk} \sum_{e=1}^C \{d_{pej}\}^T \{\omega_{pk}\}^n + \\ &+ \sum_{e=1}^C \{b_{pe}\}^T \{v_{pi,F}\}^n \end{aligned} \quad (27)$$

and for the vorticity kinetics:

$$\begin{aligned} c(\xi) \omega_{pi}(\xi) + \sum_{e=1}^E \{H_{pe}\}^T \{\omega_{pi}\}^n &= \frac{1}{\nu_{p_e}} \sum_{e=1}^E \{G_{pe}\}^T \left\{ \nu_{p_e} \frac{\partial \omega_{pi}}{\partial n} - \omega_{pi} v_{pn} + \omega_{pn} v_{pi} \right\}^n + \\ &+ \frac{1}{\nu_{p_e}} \sum_{e=1}^C \{D_{pej}\}^T \{\omega_{pi}\}_{pj}^n + \\ &+ \frac{1}{\nu_{p_e} \Delta \tau} \sum_{e=1}^C \{B_{pe}\}^T \{\omega_{pi,F}\}^n + \\ &+ \frac{1}{\nu_{p_e} \Delta \tau} \sum_{e=1}^C \{B_{pe}\}^T \{\omega_{pi}\}^n - \\ &- \frac{1}{\nu_{p_e} \varepsilon_s \Delta \tau} \sum_{e=1}^C \{B_{pe}\}^T \{\omega_{pi} \varepsilon_{p,F}\}^n \mp \\ &\mp \frac{\beta}{\rho_p \varepsilon_p} \sum_{e=1}^C \{B_{pe}\}^T \{\omega_f - \omega_s\}^n \end{aligned} \quad (28)$$

using superscript  $T$  to denote the transposition.

The plane kinematics ( $i,j=1,2$ ) can be given by the following statement based on Eqn. (27):

$$\begin{aligned} c(\xi) v_{pi}(\xi, \tau_F) + \sum_{e=1}^E \{h_{pe}\}^T \{v_{pi}\}^n &= \sum_{e=1}^E \{g_{pe}\}^T \left\{ \frac{\partial v_{pi}}{\partial n} + e_{ij} \omega_{pj} n_j \right\}^n - \\ &- e_{ij} \sum_{e=1}^C \{d_{pej}\}^T \{\omega_{pj}\}^n + \\ &+ \sum_{e=1}^C \{b_{pe}\}^T \{v_{pi,F}\}^n \end{aligned} \quad (29)$$

The plane vorticity kinetics reads:

Postopek izračunavanja integralov in zapis diskretiziranih integralskih enačb je običajen in je podrobno opisan v [6] in [8].

### 3.2 Postopek reševanja vezanih sistemov enačb

Zapisana sistema enačb kinematike, enačba (29), ter kinetike plinaste in trdne sestavine, enačba (30), dvofaznega dvoestavinskega lebdečega sloja, povezana z enačbo za izračun prostorninskega deleža sestavine (11), sestavljata močno nelinearen sistem enačb, katerih rešitev poiščemo na iterativem način. Postopek je naslednji:

(F - plinasta sestavina, S - trdna sestavina)

- 1.F Pričnemo z začetnimi predpostavljenimi vrednostmi vrtinčnosti plinaste sestavine.
- 1.S Pričnemo z začetnimi predpostavljenimi vrednostmi vrtinčnosti trdne snovi.
- 2.F Kinematika plinaste sestavine:
  - (a) rešitev implicitnega sistema za robne vrednosti hitrosti oziroma vrednosti normalnih odvodov hitrosti plinaste sestavine,
  - (b) transformacija novih funkcijskih vrednosti plinaste sestavine iz vozlišč elementov v vozlišča celic,
  - (c) določitev novih vrednosti vrtinčnosti plinaste sestavine na robu,
  - (d) določitev novih matrik kinetike plinaste sestavine, če se nespremenljivi del hitrostnega vektorja plinaste sestavine spremeni za več od predpisane tolerance.
- 2.S Kinematika trdne snovi:
  - (a) rešitev implicitnega sistema za robne vrednosti hitrosti oziroma vrednosti normalnih odvodov hitrosti trdne snovi,
  - (b) transformacija novih funkcijskih vrednosti trdne snovi iz vozlišč elementov v vozlišča celic,
  - (c) določitev novih vrednosti vrtinčnosti trdne snovi na robu,
  - (d) določitev novih matrik kinetike trdne snovi, če se nespremenljivi del hitrostnega vektorja trdne snovi spremeni za več od predpisane tolerance.
- 3.F+S Določitev prostorninskih deležev plinaste in trdne sestavine.
- 4.F Kinetika plinaste sestavine:
  - (a) rešitev implicitnega sistema za neznane vrednosti normalnih odvodov vrtinčnosti plinaste sestavine in notranjih območnih vrednosti vrtinčnosti plinaste sestavine,
  - (b) transformacija novih funkcijskih vrednosti plinaste sestavine iz vozlišč elementov v vozlišča celic.
- 4.S Kinetika trdne snovi:
  - (a) rešitev implicitnega sistema za neznane vrednosti normalnih odvodov vrtinčnosti trdne snovi in notranjih območnih vrednosti vrtinčnosti trdne snovi,
  - (b) transformacija novih funkcijskih vrednosti trdne snovi iz vozlišč elementov v vozlišča celic.

The procedure is standard and can be seen in detail in [6] and [8].

### 3.2 Solution procedure

The kinematics relations, Eqn. (29), and the vorticity transport equations, Eqn. (30), for both phases motion are coupled in two sets of non-linear equations. These two sets are related to each other by Eqn. (11), which is used to compute the volume fraction of the fluid phase knowing the velocity fields of both components. In order to obtain a solution of the fluid and solid particles motion problem a sequential computational algorithm was developed. The main steps in this algorithm are:

- (F - gas phase, S - solid phase)
- 1.F Start with initial values for the fluid-phase vorticity distribution.
  - 1.S Start with initial values for the solid-phase vorticity distribution.
  - 2.F Fluid-phase kinematic computational part:
    - (a) solve implicit sets for boundary fluid-phase velocity or velocity normal flux values,
    - (b) transform new values from element nodes to cell nodes,
    - (c) determine new boundary fluid-phase vorticity values,
    - (d) compute new fluid-phase matrices for the kinetics if the constant fluid-phase velocity vector is perturbated more than the prescribed tolerance.
  - 2.S Solid-phase kinematic computational part:
    - (a) solve implicit sets for boundary solid-phase velocity or velocity normal flux values,
    - (b) transform new values from element nodes to cell nodes,
    - (c) determine new boundary solid-phase vorticity values,
    - (d) compute new solid-phase matrices for the kinetics if the constant solid-phase velocity vector is perturbated more than the prescribed tolerance.
  - 3.F+S Determine volume fraction of the fluid and solid-phase.
  - 4.F Fluid-phase vorticity kinetic computational part:
    - (a) solve implicit set for unknown boundary fluid-phase vorticity flux and internal domain fluid-phase vorticity values,
    - (b) transform new values from element nodes to cell nodes.
  - 4.S Solid-phase vorticity kinetic computational part:
    - (a) solve implicit set for unknown boundary solid-phase vorticity flux and internal domain solid-phase vorticity values,
    - (b) transform new values from element nodes to cell nodes.

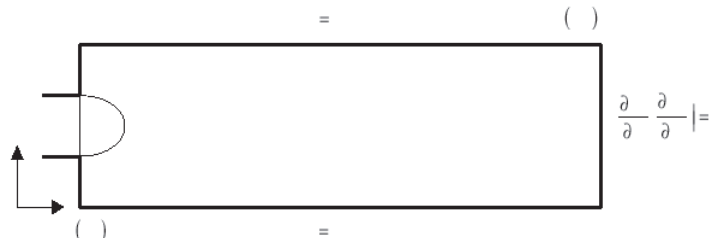
5.F Podsprostitev vrtinčnosti plinaste sestavine in preverjanje konvergencije. Če je konvergenčni kriterij izpolnjen z izračuni, prenehamo, sicer se vrnemo na korak 2.F.

5.S Podsprostitev vrtinčnosti trdne snovi in preverjanje konvergencije. Če je konvergenčni kriterij izpolnjen z izračuni, prenehamo, sicer se vrnemo na korak 2.S.

#### 4 TESTNI PRIMERI

##### 4.1 Enofazni enosestavinski tok v kanalu z nenadno simetrično razširitvijo

Tok v kanalu z nenadno simetrično razširitvijo je podoben toku v kanalu s stopnico, saj tudi tukaj pride do pojava recirkulacije pri večjih vrednostih Reynoldsovega števila. Posebnost problema je obnašanje toka pri večjih vrednostih Reynoldsovega števila, ko se prvotno simetrični recirkulacijski coni začneta razlikovati po dolžini. V našem primeru smo simulirali enofazni enosestavinski tok v kanalu z nenadno simetrično razširitvijo za vrednost Reynoldsovega števila  $Re=56$ , ki je dobro dokumentiran z eksperimentalnimi podatki (Durst [5]). Tok v kanalu z nenadno simetrično razširitvijo označuje preprosta geometrijska oblika z vstopnim območjem, omejenim na  $1/3$  višine kanala. Locirano je na sredini kanala, kar kaže slika 1, kjer so prikazani tudi robni pogoji in izmere kanala.



Sl. 1. Enofazni tok skozi nenadno simetrično razširitev. Geometrija in robni pogoji.  
Fig. 1. Single-phase symmetric sudden expansion flow. Geometry and boundary conditions.

Predpisani vstopni profil hitrosti je enak izmerjenemu [5] in nekoliko odstopa od paraboličnega profila razvitega laminarnega toka. Pri izstopu iz kanala smo predpisali normalne odvode hitrosti. Prikazani rezultati temeljijo na diskretizaciji računskega območja z  $20 \times 18$  podobmočji z razmerjem najdaljši/najkrajši element = 2 v koordinatnih smerih  $x$  in  $y$ . Zaradi nenadne razširitev se pojavitva recirkulacijskih območij ob zgornji in spodnji steni kanala, ki se z večanjem vrednosti Reynoldsovega števila povečujeta. Hitrostno polje je simetrično, kar je razvidno tudi iz eksperimentalnih rezultatov. V začetku kanala je še viden vpliv recirkulacije, medtem ko se proti izstopu vzpostavi razviti profil hitrosti. Hitrostne profile za ustaljeno rešitev smo primerjali z meritvami Dursta, Mellinga in Whitelawa [5].

5.F Relax fluid-phase vorticity values and check the fluid-phase convergence. If convergence criterion is satisfied, then stop; otherwise, go to step 2.F.

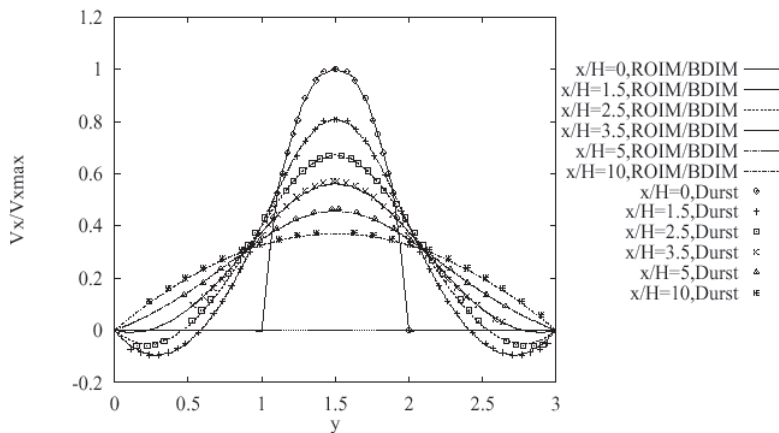
5.S Relax solid-phase vorticity values and check the solid-phase convergence. If convergence criterion is satisfied, then stop; otherwise, go to step 2.S.

#### 4 TEST EXAMPLES

##### 4.1 Single-phase symmetric sudden expansion flow

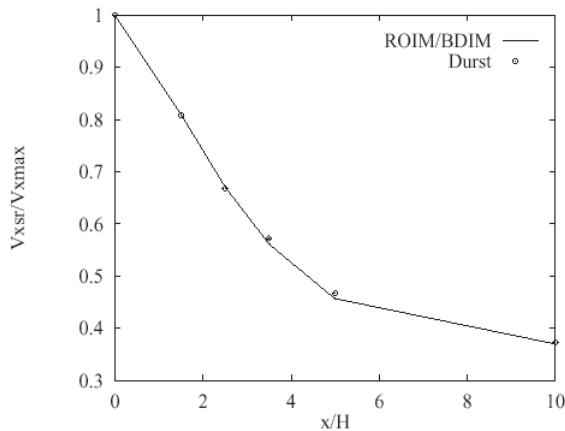
Because of the recirculation zones at larger values of Reynolds number flow downstream of the expansion a plane symmetric sudden expansion flow is similar to the backward-facing step flow. The flow is symmetric at sufficiently low values of the Reynolds number based on the step height and maximum inlet velocity. It becomes asymmetric as the Reynolds number is increased beyond the critical value. Our results were obtained at a Reynolds number of 56, which ensures the symmetric flow and enables us to compare the numerical results with the experimental values of Durst [5]. The geometry is simple with the inlet region constituting  $1/3$  of the channel height based in the middle of the channel. The geometry and boundary conditions are shown in Figure 1.

The prescribed inlet velocity profile is exactly equal to the measured one [5], and differs only a little from the parabolic profile of fully developed laminar flow. At the outlet normal velocity profiles are prescribed. The discretization consists of  $20 \times 18$  subdomains with a ratio of 2 between the longest and the shortest element. The calculated separation regions behind the expansion are, as reported by [5], of equal length, leading to the fully developed, parabolic profile far downstream. The numerical results are compared to the experimental values of Durst, Melling and Whitelaw [5].



Sl. 2. Enofazni tok skozi nenadno simetrično razširitev. Primerjava z eksperimentalnimi vrednostimi vzdolž toka na različnih oddaljenostih od razširitev.

Fig. 2. Single-phase symmetric sudden expansion flow. Comparison with experimental data at different distances downflow the expansion.



Sl. 3. Enofazni tok skozi nenadno simetrično razširitev. Primerjava z eksperimentalnimi vrednostimi vzdolž toka v sredini kanala.

Fig. 3. Single-phase symmetric sudden expansion flow. Comparison with experimental data along the horizontal line through the center of the channel.

Slika 2 prikazuje primerjavo izračunanih hitrostnih profilov z izmerjenimi na različnih oddaljenostih od nenačne razširitev kanala  $X/H = 0, 1.5, 2.5, 3.5, 5$  in  $10$ , pri čemer  $H$  označuje višino stopnice. Na sliki 3 je prikazana primerjava največjih hitrosti vzdolž simetrijske osi kanala.

#### 4.2 Dvofazni dvoestavinski tok v navpičnem kanalu

Namen raziskave je s predlagano numerično shemo ROIM simulirati vpliv različnih koeficientov medfazne izmenjave gibalne količine, kombiniranih z različnimi Stokesovimi hitrostmi trdnih delcev na hitrostni polji obeh sestavin. Geometrijska oblika in robni pogoji zastavljenega problema so prikazani na sliki 4.

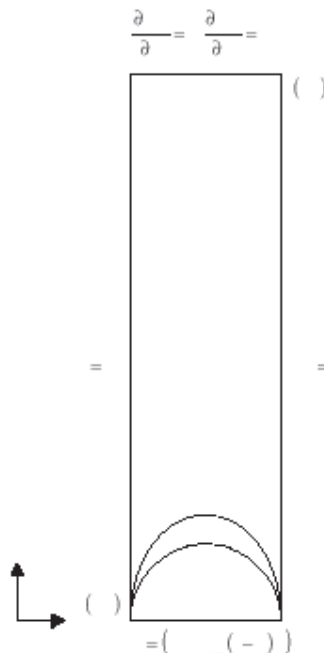
Pri vstopu v cev smo predpisali različne parabolične hitrostne profile. V prvem delu izračunov smo za sestavino 1 (plin) pri vstopu v kanal predpisali parabolo z največjo vstopno hitrostjo  $v_{fj\text{ maks}} = 1 \text{ m/s}$

Figure (2) shows the comparison at different distances downflow the expansion  $X/H = 0, 1.5, 2.5, 3.5, 5$  in  $10$ , where  $H$  denotes the height of the step. In Figure 3 the maximum velocity values are shown along the centreline of the channel.

#### 4.2 Two-phase two-component flow in the vertical channel

The aim of the research was to establish with the proposed BDIM numerical scheme the influence of different drag coefficients combined with different terminal velocities of solid phase on the velocity fields of both components. The geometry and boundary conditions for the investigated two-phase two-component vertical channel flow are presented in Figure 4.

Different parabolic velocity profiles were prescribed at the inlet. In the first set of calculations for the phase 1 (gas) the parabolic inlet velocity profile with  $v_{fj\text{ max}} = 1 \text{ m/s}$  was defined. For the phase 2 (solid



Sl. 4. Ravninski dvo fazni dvosestavinski tok med navpičnima ploščama. Geometrija in robni pogoji.  
Fig. 4. Two-phase two-component vertical channel flow. Geometry and boundary conditions.

in za sestavino 2 (trdna snov) parabolo z največjo vstopno hitrostjo  $v_{sy\ maks} = 0,5$  m/s. V drugem delu izračunov smo zmanjšali največjo vstopno hitrost trdne sestavine na  $v_{sy\ maks} = 0,4$  m/s in primerjali potek hitrostnih profilov vzdolž navpičnice skozi središče kanala. Zdrs sestavin na trdnih stenah ni bil mogoč. Pri izstopu iz kanala smo predpisali normalne odvode vektorjev hitrosti. Po celotnem računskem območju smo upoštevali realno vrednost koeficiente medfazne izmenjave gibalne količine. Izvedli smo izračune z vrednostmi od  $\beta = 10$  kg/m<sup>3</sup>s do  $\beta = 30$  kg/m<sup>3</sup>s. Ustaljeno analizo smo simulirali s prehodno za zelo velik časovni korak ( $\Delta\tau = 10^{15}$ ). Konvergenčni kriterij vseh izračunov je bil  $10^{-4}$ .

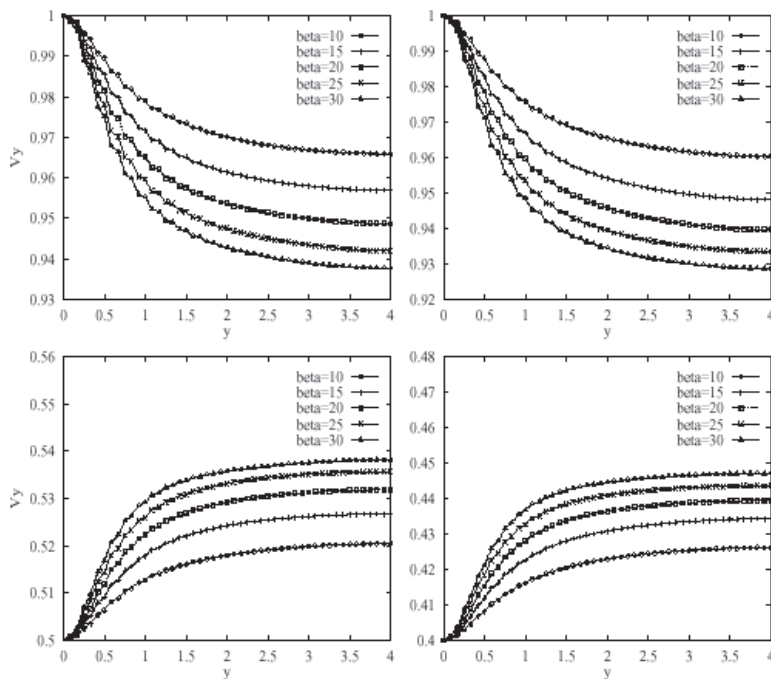
Slike 5 in 6 prikazujeta navpično komponento vektorjev hitrosti vzdolž navpične črte skozi središče kanala. Oblika hitrostnih profilov je močno odvisna od koeficiente trenja  $\beta$ . Rezultati izračunov na sliki 5 kažejo odvisnost hitrosti od vrednosti koeficiente trenja  $\beta$  pri izbrani Stokesovi hitrosti posameznega trdnega delca, medtem ko slika 6 prikazuje primerjavo hitrostnih profilov pri izbranem trenju med sestavinama in spremenljajoči se Stokesovi hitrosti trdnih delcev. V obeh primerih je jasno razvidno, da se z večanjem koeficiente trenja  $\beta$  hitrostni profili obeh sestavin vedno bolj približujejo drug proti drugemu. Prav tako pričakovano je zmanjševanje največjih hitrosti obeh sestavin vzdolž srednice kanala zaradi povečevanja Stokesove hitrosti trdnih delcev.

Simuliranja manjšajoče se hitrosti sestavine 1 in večajoče se hitrosti sestavine 2 smo za oba primera vstopnih pogojev izvedli na različnih računskih mrežah. Konvergenco rezultatov z zgoščevanjem računske mreže podajata preglednici 1 in 2.

phase) the maximum inlet velocity was set to the value of  $v_{sy\ max} = 0.5$  m/s. In the second part of the calculations the maximum inlet velocity of phase 2 was decreased to the  $v_{sy\ max} = 0.4$  m/s. The velocity profiles along the vertical line through the centre of the channel were compared to each other. No-slip conditions on the rigid walls were prescribed for both phases motion. Normal velocity fluxes at the outlet were given as known quantities. All over the computational domain a realistic value of the interphase momentum transfer coefficient was given. Calculations with different values of drag coefficient between  $\beta=10$  kg/m<sup>3</sup>s and  $\beta=30$  kg/m<sup>3</sup>s were made. Steady-state analysis was simulated by a transient one for one very large time step ( $\Delta\tau = 10^{15}$ ). The convergence criteria for all runs were  $10^{-4}$ .

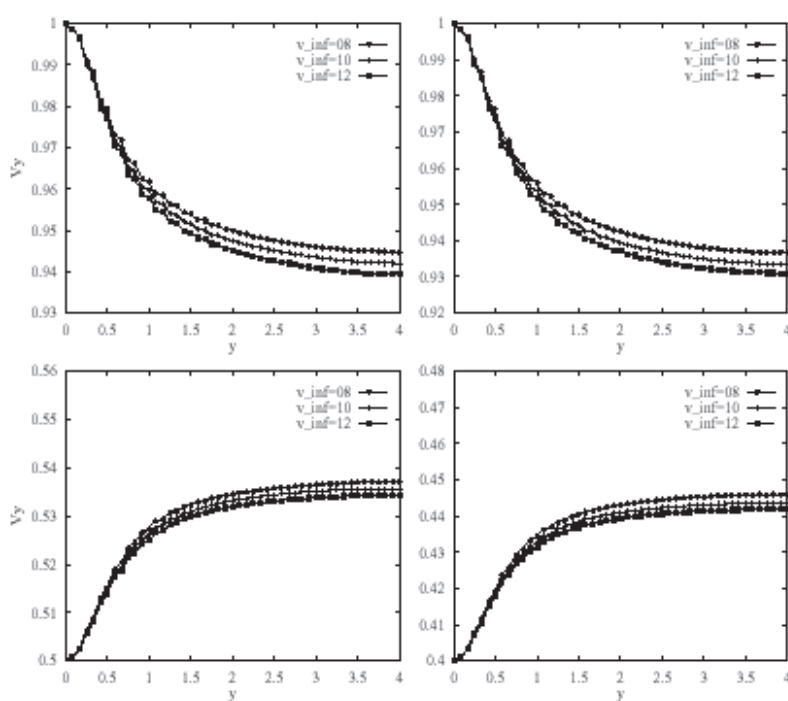
Figures 5 and 6 show the vertical component of the velocity vectors along the vertical line through the centre of the channel. The shape of the velocity profiles strongly depends on the drag coefficient  $\beta$ . The results in Figure 5 show the influence of the drag coefficient on the velocity fields at a fixed Stokes velocity of a single solid particle. On the other hand, Figure 6 shows the results at a fixed drag coefficient and variable Stokes velocity. In both cases one can see that the velocity profiles are moving closer to each other with an increasing interphase momentum exchange coefficient. Also, a decrease of the maximum velocities due to the increasing Stokes velocity was expected.

Simulations of the decreasing velocity of phase 1 and the increasing velocity of phase 2 were also carried out on different mesh densities. The convergence of the results is given in Tables 1 and 2.



Sl. 5. Vpliv koeficienta medfazne izmenjave gibalne količine  $\beta$  na navpično komponento vektorja hitrosti sestavine 1 (zgoraj) in sestavine 2 (spodaj) vzdolž srednice kanala na mreži s  $6 \times 24$  podobmočji ( $v_{\text{vstop maks } 1} = 1 \text{ m/s}$ ,  $v_{\text{vstop maks } 2} = 0.5 \text{ m/s}$  (levo),  $v_{\text{vstop maks } 2} = 0.4 \text{ m/s}$  (desno),  $v_\infty = 10 \text{ m/s}$ ).

Fig. 5. Two-phase two-component vertical channel flow. Influence of interphase momentum exchange coefficient  $\beta$  on vertical component of phase 1 (upper line) and phase 2 (lower line) along the vertical line through the center of the channel at discretization  $6 \times 24$  subdomains ( $v_{\text{inlet max } 1} = 1 \text{ m/s}$ ,  $v_{\text{inlet max } 2} = 0.5 \text{ m/s}$  (left),  $v_{\text{inlet max } 2} = 0.4 \text{ m/s}$  (right),  $v_\infty = 10 \text{ m/s}$ ).



Sl. 6. Vpliv Stokesove hitrosti sestavine 2  $v_\infty$  na navpično komponento vektorja hitrosti sestavine 1 (zgoraj) in sestavine 2 (spodaj) vzdolž srednice kanala na mreži s  $6 \times 24$  podobmočji

( $v_{\text{vstop maks } 1} = 1 \text{ m/s}$ ,  $v_{\text{vstop maks } 2} = 0.5 \text{ m/s}$  (levo),  $v_{\text{vstop maks } 2} = 0.4 \text{ m/s}$  (desno),  $\beta = 25 \text{ kg/m}^3\text{s}$ ).

Fig. 6. Two-phase two-component vertical channel flow. Influence of Stokes velocity of phase 2  $v_1$  on vertical component of phase 1 (upper line) and phase 2 (lower line) along the vertical line through the center of the channel at discretization  $6 \times 24$  subdomains

( $v_{\text{inlet max } 1} = 1 \text{ m/s}$ ,  $v_{\text{inlet max } 2} = 0.5 \text{ m/s}$  (left),  $v_{\text{inlet max } 2} = 0.4 \text{ m/s}$  (right),  $\beta = 25 \text{ kg/m}^3\text{s}$ ).

Preglednica 1: Ravninski dvofazni dvosestavinski tok med navpičnima ploščama. Primerjava navpične komponente izstopne hitrosti  $v_{py}$  v odvisnosti od diskretizacije ( $v_{vstop maks 1} = 1 \text{ m/s}$ ,  $v_{vstop maks 2} = 0,5 \text{ m/s}$ ,  $\beta = 25 \text{ kg/m}^3\text{s}$ ,  $v_\infty = 10 \text{ m/s}$ ).

Table 1: Two-dimensional two-phase two-component vertical channel flow. Comparison of vertical component of the outlet velocity  $v_{py}$  regarding to the mesh density ( $v_{inlet max 1} = 1 \text{ m/s}$ ,  $v_{inlet max 2} = 0.5 \text{ m/s}$ ,  $\beta = 25 \text{ kg/m}^3\text{s}$ ,  $v_\infty = 10 \text{ m/s}$ ).

mreža/ mesh	nestančna 1/ phase 1	nestančna 2/ phase 2
6 x 12	0.946	0.534
6 x 16	0.943	0.535
6 x 20	0.942	0.535
6 x 24	0.942	0.536
6 x 28	0.942	0.536
6 x 40	0.942	0.536
12 x 40	0.942	0.536

Preglednica 2: Ravninski dvofazni dvosestavinski tok med navpičnima ploščama. Primerjava navpične komponente izstopne hitrosti  $v_{py}$  v odvisnosti od diskretizacije ( $v_{vstop maks 1} = 1 \text{ m/s}$ ,  $v_{vstop maks 2} = 0,4 \text{ m/s}$ ,  $\beta = 25 \text{ kg/m}^3\text{s}$ ,  $v_\infty = 10 \text{ m/s}$ ).

Table 2: Two-dimensional two-phase two-component vertical channel flow. Comparison of vertical component of the outlet velocity  $v_{py}$  regarding to the mesh density ( $v_{inlet max 1} = 1 \text{ m/s}$ ,  $v_{inlet max 2} = 0.4 \text{ m/s}$ ,  $\beta = 25 \text{ kg/m}^3\text{s}$ ,  $v_\infty = 10 \text{ m/s}$ ).

mreža/ mesh	nestančna 1/ phase 1	nestančna 2/ phase 2
6 x 12	0.935	0.442
6 x 16	0.934	0.443
6 x 20	0.934	0.443
6 x 24	0.934	0.444
6 x 28	0.933	0.444
6 x 40	0.933	0.444
12 x 40	0.933	0.444

## 5 SKLEP

V prispevku je prikazan razvoj robno-območne integralske metode za numerično simuliranje dvofaznih dvosestavinskih tokov plin - trdni delci. Uporabili smo hitrostno-vrtinčno formulacijo dopolnjenih Navier-Stokesovih enačb. Vodilne enačbe smo poenostavili z uvedbo predpostavke o nespremenljivem prostorninskem deležu sestavine v podobmočju v iteraciji numeričnega algoritma. Zaradi nezvezne porazdelitve hitrosti na mejah med makroelementi smo predpisali primerne pogoje vmesnega roba. Za sklenitev zapisanega sistema kinematičnih in kinetičnih enačb gibanja sestavin lebdečega sloja, smo uporabili dodatno enačbo za izračun prostorninskega deleža, ki je izpeljana iz teorije gnanega toka dvofaznih tokov. Prednost predstavljenih shem na podlagi robno območne integralske metode v primerjavi z običajnimi, ki brez izjeme temeljijo na postopkih končnih razlik, končnih elementov in kontrolnih prostornin, je zmanjšano število dodatnih modelov za določitev navideznih lastnosti trdne snovi. Pravilnost delovanja razvite sheme smo najprej potrdili na primeru enofaznega toka v kanalu z nenadno simetrično razširitvijo. Vplive

## 5 CONCLUSION

The boundary domain integral method was used to simulate two-dimensional two-phase two-component gas-solid flow. The velocity-vorticity approach in combination with modified Navier-Stokes equations was employed. The set of governing equations was simplified under the assumption that the volume fraction of each component is constant in each macroelement within one iteration. The discontinuous velocity distribution on the interfaces between the subdomains was overcome with the prescription of the appropriate interface macroelement boundary conditions. An additional equation to compute the volume fraction of the fluid phase was obtained from the drift-flux theory. The advantage of the proposed scheme is a reduced number of gas-solid physical models. The numerical model was first validated on single-phase test examples such as single-phase symmetric sudden expansion flow. Finally, the influence of the drag force and the terminal

koeficiente medfazne izmenjave gibalne količine in vpliv različnih Stokesovih hitrosti trdnih delcev na hitrostni polji sestavin smo testirali na primeru dvofaznega dvoestavinskega toka v navpičnem kanalu.

velocity of the solid phase on both components velocity fields was tested for the case of two-phase two-component vertical channel flow.

## 6 SIMBOLI 6 SYMBOLS

prostorninski delež sestavine	$\varepsilon_p$	volume fraction of the phase
i-ta trenutna komponenta hitrosti sestavine	$v_{pi}$	i-th instantaneous phase velocity component
gostota sestavine	$\rho_p$	density of the phase
i-ta koordinata	$x_i$	i-th coordinate
snovski oziroma Stokesov odvod	$D/D\tau$	substantial or Stokes derivative
tenzor viskoznih napetosti sestavine	$S_{pij}$	viscous stress tensor of the phase
gravitacijski pospešek	$g_i$	gravity acceleration
termodynamični tlak	$p$	thermodynamic pressure
navidezni tlak trdne snovi	$p_s^*$	solids pressure
koeficient medfazne izmenjave gibalne količine	$\beta$	interphase momentum transfer coefficient
i-ta trenutna komponenta vrtinčnosti	$\omega_{pi}$	i-th instantaneous phase vorticity component
Stokesova hitrost trdnih delcev	$v_\infty$	Stokes velocity of solid particles
koeficient	$n$	coefficient
sprostivitveni parameter v kinematični enačbi sestavine	$\alpha_p$	relaxation parameter in kinematic equation of the phase
nespremenljiva kinematična strižna viskoznost sestavine	$\nu_{p0}$	constant phase kinematic shear viscosity
nespremenljiva kinematična normalna viskoznost sestavine	$\kappa_{p0}$	constant phase kinematic bulk viscosity
permutacijski enotski tenzor	$e_{ijk}$	permutation unit tensor

## 7 LITERATURA 7 REFERENCES

- [1] Anderson, T.B., R. Jackson. (1967) A fluid mechanical description of fluidized beds. *Ind Engng Chem Fundam* 6, 527-539.
- [2] Bird, R.B., W.E. Stewart, E.N. Lightfoot (1960) Transport phenomena. New York. *John Wiley & Sons*.
- [3] Boemer, A., Qi, H., Renz, U., Vasquez, S., Boysan, F. (1995) Eulerian computation of fluidized bed hydrodynamics - A comparison of physical models. *Proceedings of the 13th International Conference on Fluidized Bed Combustion*, Orlando, 775-781.
- [4] Chapman, S., T.G. Cowling (1970) The mathematical theory of non-uniform gases. Cambridge, *Cambridge University Press*.
- [5] Durst, F., A. Melling, J.H. Whitelaw (1974) Low Reynolds number flow over a plane symmetric sudden expansion. *J. Fluid Mechanics*, 64(1), 111-128.
- [6] Požarnik, M. (2000) Doktorska disertacija, Univerza v Mariboru.
- [7] Richardson, J.F., W.N. Zaki (1954) Sedimentation and fluidization: Part I. *Trans Instn Chem Engrs* 32, 35-53.
- [8] Škerget, L., Z. Rek (1995) Boundary-domain integral method using a velocity-vorticity formulation. *Eng Anal Bound Elem* 15, 359-370.
- [9] Wallis, G.B. (1969) One-dimensional Two-phase Flow. *McGraw-Hill*.

Naslov avtorjev: dr. Matej Požarnik  
 prof.dr. Leopold Škerget  
 Fakulteta za strojništvo  
 Univerza v Mariboru  
 Smetanova 17  
 2000 Maribor  
 matej.pozarnik@uni-mb.si  
 leo@uni-mb.si

Authors' Address: Dr. Matej Požarnik  
 Prof.Dr. Leopold Škerget  
 University of Maribor  
 Faculty of Mechanical Eng.  
 Smetanova 17  
 2000 Maribor, Slovenia  
 matej.pozarnik@uni-mb.si  
 leo@uni-mb.si

Prejeto:  
 Received: 5.9.2001

Sprejeto:  
 Accepted: 29.3.2002